JOURNAL OF SOLID STATE CHEMISTRY 29, 27–34 (1979)

Electrical Conductivities of Potassium Ferrites Doped with Divalent Metal Oxide

TAKEHIKO TAKAHASHI AND KATSUMI KUWABARA

Department of Applied Chemistry, Faculty of Engineering, Nagoya University, Nagoya 464, Japan

Received June 12, 1978; in revised form September 5, 1978

The electronic and ionic conduction in three kinds of potassium ferrites with β-alumina structure was studied. Undoped ferrite, $K_2O{\cdot}6Fe_2O_3$, prepared by sintering at 1400°C after prefiring a mixture of potassium carbonate and ferric oxide, was a mixed conductor with about 1% ionic conduction and predominantly electronic conduction. The nickel- or zinc-doped potassium ferrite showed decreasing conductivity in the range of a single phase as the content of dopant increased. Variations of the electronic conduction in the doped potassium ferrites were assigned to changes of ferrous ion concentration accompanied by structural changes in the spinel-like blocks. Potassium ion conductivities of the three sorts of samples were estimated from the total conductivities and the transport numbers obtained by dc-polarization technique and electrolysis method. The decreases of the ionic conductivities were explained by narrowing of the alkali–oxygen slot caused by doping.

1. Introduction

Potassium ferrite was found in connection with a study on magnetoplumbite $MeO{\cdot}6M_2O_3$ (Me = Ca, Sr, Ba, Pb; M = Al, Fe) (*1*). In earlier studies on potassium ferrite (*2–4*) it was shown that the compound crystallized in a hexagonal layer structure and had a composition of $K_2O{\cdot}11Fe_2O_3$ analogous to β-alumina, $Na_2O{\cdot}11Al_2O_3$. Ohtsubo and Yamaguchi (*5*) investigated the compound in the K_2CO_3–Fe_2O_3 system in detail using differential thermal analysis and X-ray diffraction. They pointed out that the chemical composition of the stable phase of potassium ferrite was not $K_2O{\cdot}11Fe_2O_3$ but $K_2O{\cdot}7Fe_2O_3$. Other compositions such as $K_2O{\cdot}6Fe_2O_3$ (*6*) and $K_2O{\cdot}5Fe_2O_3$ (*7*) were reported in the K_2O–Fe_2O_3 system. The present authors (*8*) examined the region of potassium ferrite formation and indicated a phase diagram of the $KFeO_2$–Fe_2O_3 system on the basis of the results of melting-point observation, X-ray diffraction, and electrical conductivity measurements. According to the phase diagram, potassium ferrite is a nonstoichiometric compound in the range of Fe_2O_3/K_2O = 6–6.8.

The dc conductivities of potassium ferrites in both single crystal and polycrystalline form were measured first by Roth and Romanczuk (*9*). Recently, in a series of studies of potassium ferrite, Dudley and coworkers (*10, 11*) measured the electronic and ionic conductivities of the nonstoichiometric potassium ferrite phase as a function of temperature and potassium ion concentration. Potassium ion conduction in polycrystalline potassium ferrites $K_2O{\cdot}(6-x)Fe_2O_3{\cdot}xMO$ (M = Zn, Mg, Ni) was also studied qualitatively by the present authors (*12*). In the present work, the electronic and

0022-4596/79/070027-08$02.00/0

ionic conduction in potassium ferrite with a new formula of $(1+x/2)\,K_2O{\cdot}6Fe_2O_3{\cdot}xMeO$ (Me = Ni, Zn) was reinvestigated from a structural point of view as a function of temperature and content of the divalent metal ion.

2. Experimental

2.1. Materials

Potassium carbonate and ferric oxide from ferrous oxalate were ground together in a mole ratio of $Fe_2O_3/K_2O = 6$. Tablets of 13-mm diameter and 3-mm thickness pressed at 1 kbar were fired at 950°C for 15 hr in air. The calcined tablets were ground, pressed isostatically in a rubber fingersack at about 3 kbar, embedded in the powder of the same composition, and heated at 1400°C for 1 hr in air. The resulting tablet of 7-mm diameter and 15-mm length had an apparent density of about $4\,g\,cm^{-3}$ which was 95% theoretical.

Divalent metal oxide, MeO (Me = Ni or Zn), was added to potassium ferrite in the formula of $(1+x/2)K_2O{\cdot}6Fe_2O_3{\cdot}xMeO$. Zinc oxide was guaranteed grade and nickel oxide was prepared from nickel hydroxide by thermal decomposition at 1200°C for 3 hr in nitrogen flow. The starting powders were mixed in an agate mortar using ethanol as a dispersing reagent. After the removal of the alcohol at 100°C, the dried powders were treated in the same procedure as in the case of the undoped potassium ferrite.

Alkali vaporization could be unavoidable during the heating process of the samples. Weight losses of the tablets, however, could be minimized within 1 wt % compared with the starting compositions by the above-mentioned embedding technique. On the basis of these results, all the following compositions are described by the starting ones. The tablets thus obtained was ground to fine powder for X-ray diffraction study which was carried out with cobalt target, iron filter, and scintillation counter. In the case of the measurement of lattice parameters silicon powder was used as an inner standard material.

2.2. Measurement of Conductivity

The surface of the sintered tablet was polished by use of emery paper to prepare a specimen 7–8 mm in diameter and 2–15 mm in length. The electrode used was gold foil and the specimen was held by compression in a stainless-steel frame. The temperature dependence of the total conductivity of the sample was examined over the region from 100 to 500°C in air. The conductivity was measured using an impedance bridge at 10 kHz because of its small dependence on frequency.

In order to examine whether the conduction was ionic or electronic, the dc polarization technique was applied as described in previous papers (*12, 13*). In this case, gold foil was used as a blocking electrode. A direct current was passed for a few minutes under the condition of an applied voltage lower than the decomposition voltage of the sample. If the measuring voltage ascends continuously from the start, the conduction is chiefly ionic, and if it rises instantaneously on switching and then increases gradually with time, the conduction can be judged to be a mixture of ionic and electronic. The ionic and electronic parts are approximated by the equations $t_i = (V_s - V_i)/V_s$ or V_r/V_s and $t_e = V_i/V_s$ respectively, where V_i is the initial standing voltage of 0.00–6.50 mV, V_s the apparent steady-state voltage of 0.50–10.0 mV and V_r the residual voltage of 0.00–10.0 mV.

For the determination of mobile species, the transport number of the sample was measured by the electrolysis technique. A pellet of the sample was sandwiched between two potassium ferrite disks which were available for the electrode material described in the following section.

3. Results and Discussion

3.1. Conductivity of Undoped Potassium Ferrite, $K_2O \cdot 6Fe_2O_3$

Typical conductivity of undoped potassium ferrite is shown in Fig. 1. The conductivity plot is not linear but slightly curved as in the plot indicated by Roth and Romanczuk (*9*). The conduction was examined by the polarization and electrolysis techniques. In the former case, for example, when the current passed was 3.0 mA at 300°C, $V_i = 7.8$, $V_s = 8.0$, and $V_r = 0.1$ mV, so $t_i = 0.2/8.0 = 0.02$ or $0.1/0.8 = 0.01$. In the latter technique, the weight changes of the same sample at 300°C were −8.6 mg at the anode-side and +12.2 mg at the cathode-side tablet, while the weight changes calculated from the amount of electricity (1490 C), assuming that the potassium ion transport number is unity, were −600 and +600 mg at the anode and the cathode, respectively. The ratio of these weight changes, 0.012 or 0.014, would be equal to the potassium ion transport number which was nearly equal to that obtained by the dc-polarization technique.

From the total conductivity and the transport number, the potassium ion conductivity of potassium ferrite was calculated to be 1.5×10^{-2} $(\text{ohm}\cdot\text{cm})^{-1}$ at 300°C, which agreed very well with the value 1.6×10^{-2} $(\text{ohm}\cdot\text{cm})^{-1}$ obtained from the diffusion constant of potassium ferrite (*14*) and with that obtained from the measurement of transient voltages (*11*) in the order of magnitude of 10^{-2} $(\text{ohm}\cdot\text{cm})^{-1}$. These results suggested that potassium ferrite was a mixed ionic and electronic conductor containing high potassium ion conduction. It was pointed out by Roth and Romanczuk (*9*) that the electronic conduction in potassium ferrite depended on the ferrous ion concentration varied by equilibration with varying partial pressures of oxygen at temperatures above 300°C. This is the reason for deviation of the conductivities from sample to sample and from paper to paper. Therefore, strictly speaking, the total conductivity should be discussed in terms of the partial pressure of oxygen.

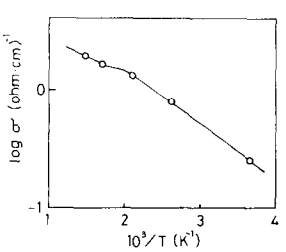

FIG. 1. Total conductivity of undoped potassium ferrite, $K_2O \cdot 6Fe_2O_3$, sintered at 1400°C for 1 hr in air.

3.2. Conductivity of $(1 + x/2)K_2O \cdot 6Fe_2O_3 \cdot xNiO$

The total conductivity of potassium ferrite doped with nickel oxide is shown in Fig. 2. The conductivity monotonically decreases from the composition of $x = 0$ to $x = 1.0$ and the slope of the curve increases with increased x. In this composition range, the samples were revealed by X-ray diffraction to have the single phase with the β-alumina structure.

The conduction in these nickel-doped potassium ferrites was mixed ionic and electronic as in undoped sample. The dc-polarization curves are shown schematically in Fig. 3. In the case of the composition $x = 0.2$, the initial voltage is nearly equal to

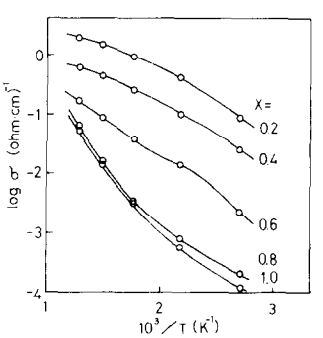

FIG. 2. Total conductivity of nickel-doped potassium ferrite, $(1 + x/2)K_2O \cdot 6Fe_2O_3 \cdot x$NiO, sintered at 1400°C for 1 hr in air.

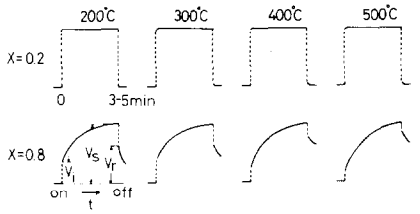

FIG. 3. The dc polarization curves of nickel-doped potassium ferrite.

the steady-state voltage at every temperature, although the ratio of the former to the latter decreases little by little with rising temperature. On the other hand, for the composition $x = 0.8$ the standing voltage decreased with rise of temperature. Table I lists the electronic and ionic transport numbers obtained from the polarization curves. It is evident from the table that the ionic part of conduction increases with the content of nickel oxide and with temperature.

As already mentioned above, potassium ferrite $K_2O{\cdot}6Fe_2O_3$ had high total conductivity and about 1% of it was assigned to the potassium ion. Therefore, undoped potassium ferrite appeared to have an ability of working as a reversible electrode to potassium ion. Hever (*15*) used both mixed sodium–potassium ferrite and a solid solution of sodium β-aluminate–ferrite as alkali-ion-reversible electrodes, and Kennedy and Sammels (*16*) substituted iron oxide for aluminium oxide in sodium β-alumina for use as a cathode for galvanic cells. This kind of electrode has not been, with the exception of sodium tungstate, used as a reversible electrode for sodium ion in sodium β-alumina (*17*).

The weight changes after the electrolysis of nickel-doped potassium ferrite are shown in Table II together with the electricity used. The increase in the nickel oxide content leads to an increase in the ratio of the observed to the calculated weight change considering only potassium ion conduction. This ratio corresponds to the potassium ion transport number which rises remarkably with the content of the dopant.

3.3. Conductivity of $(1+x/2)K_2O{\cdot}6Fe_2O_3{\cdot}xZnO$

The conductivity curve of zinc-doped potassium ferrite which has a single phase in the range $0 \leq x \leq 0.9$ is shown in Fig. 4. The conductivity decreases with increasing content of zinc oxide as in the case of nickel doping, but the former has a conductivity a

TABLE I

ELECTRONIC AND IONIC TRANSPORT NUMBERS OF $(1+x/2)K_2O{\cdot}6Fe_2O_3{\cdot}xNiO$ OBTAINED BY DC POLARIZATION CURVES

		Temperature (°C)			
x	t	200	300	400	500
0.2	t_e	1.0	>0.95	>0.95	0.95
	t_i	0	<0.05	<0.05	0.05
0.4	t_e	>0.95	>0.95	0.95	>0.90
	t_i	<0.05	<0.05	0.05	<0.10
0.6	t_e	>0.90	>0.90	0.90	>0.85
	t_i	<0.10	<0.10	0.10	<0.15
0.8	t_e	>0.35	0.35	0.20	<0.15
	t_i	<0.65	0.65	0.80	>0.85

TABLE II

THE WEIGHT CHANGES OF NICKEL-DOPED POTASSIUM FERRITE AFTER ELECTROLYSIS AT 350°C IN AIR[a]

x	Electric charge (C)	ΔW (mg)		$\Delta W_{obs}/\Delta W_{calc}$
		Obs	Calc	
0.2	2028	5.8	821	0.00_7
0.4	1332	10.4	539	0.01_9
0.6	163	9.4	66.0	0.14
0.8	36	12.0	14.6	0.82
1.0	11.3	4.6	4.6	0.99

[a]Calculated values were obtained assuming only potassium ion transport with each amount of electricity.

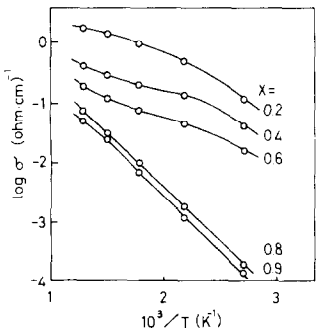

FIG. 4. Total conductivity of zinc-doped potassium ferrite, $(1+x/2)K_2O{\cdot}6Fe_2O_3{\cdot}xZnO$, sintered at 1400°C for 1 hr in air.

little higher than the latter at the same composition.

The dc-polarization curves suggested predominantly electronic conduction in the region of low content of zinc oxide while they showed ionic conduction in the high-content region. In order to confirm the behavior quantitatively, the samples were electrolyzed at several temperatures. Table III shows the resultant weight changes at 350°C. It can be seen from comparison of Table III with Table II that in the region of higher content the samples doped with zinc oxide have ionic transport numbers lower than those doped with nickel oxide.

TABLE III

THE WEIGHT CHANGES OF ZINC-DOPED POTASSIUM FERRITE AFTER ELECTROLYSIS AT 350°C IN AIR[a]

		ΔW (mg)		
x	C	Obs	Calc	$\Delta W_{obs}/\Delta W_{calc}$
0.2	720	3.3	292	0.01_1
0.4	495	12.6	200	0.06_3
0·6	309	13·7	125	0·11
0.8	51	11.9	20.7	0.58
0.9	30	9.6	12.2	0.79

[a]Calculated values were obtained assuming only potassium ion migration with each amount of electricity.

3.4. *Electronic Conduction*

Several potassium ferrites examined in this paper have been shown to be mixed ionic and electronic conductors. According to the measurements of the transport numbers, the total conductivity of the sample doped with divalent metal ions appears to decrease chiefly because of the decrease of the electronic conductivity with increased dopant content. Since the electronic conductivity is due to the presence of ferrous ion as described by earlier investigators (*9, 15*), the decrease in electronic conductivity would be due to decrease in the ferrous ion concentration. This problem is interesting in connection with a certain structural change accompanied by divalent metal doping.

The β-alumina structure contains spinel-like block. Generally in spinel-like substances XY_2O_4 (*18*), the X ions occupy fourfold coordination positions and the Y ions are in sixfold coordination positions. This arrangement is indicated as characteristic for "normal spinels (N type)." On the other hand, there is another arrangement in which the fourfold interstices are occupied by half of the Y ions, the sixfold holes by the X ions, and the other half of the Y ions are distributed at random at these positions. This arrangement may be indicated as characteristic for "inversed spinels (I type)." Iron and nickel ferrites belong to the I type and zinc ferrite to the N type.

Applying these arrangements of cations in spinels to the potassium ferrites now under consideration, differences in lattice parameters between undoped and doped samples might be estimated using ionic radii of the cations. Effective ionic radii taking into account the coordination number were presented by Shannon and Prewitt (*19*) as follows: Fe^{2+} (coordination number IV) 0.63, (VI) 0.77; Fe^{3+} (IV) 0.49, (VI) 0.645; Ni^{2+} (VI) 0.700; Zn^{2+} (IV) 0.60, (VI) 0.745 Å. In the case of nickel doping, nickel

ions would substitute for ferrous ions in the octahedral positions of the spinel-like block because of the isomorphous I type of iron and nickel ferrites. In the β-alumina structure, it is easy to calculate the edge length of the spinel-like block in the a direction corresponding directly to the lattice parameter a, while the estimation of the length in the c direction is not always simple because the c axis contains the alkali–oxygen layer as well as the spinel-like block. Therefore, the substitution of ions would result in not only the contraction of the spinel-like block but also contraction of the a axis of nickel–doped potassium ferrite. The observed lattice parameters of the sample are shown in Fig. 5. As can be seen from this figure, the increased nickel content leads to decrease in a, which agrees well with the estimation mentioned above. In addition, the substitution would also bring a relative decrease in ferrous ion concentration, so that the decrease in the electronic conductivity might be explained by the effect of the ion substitution.

In the case of zinc doping, zinc ions would enter the fourfold coordination sites to replace ferric ions because of N-type spinel of zinc ferrite. The replacement of ions would lead to the expansion of the spinel-like block due to the different ionic radii. On the other hand, from the condition of electrical neutrality, ferrous ions in the sixfold coordination positions would have to be oxidized to ferric ions which are smaller than ferrous ions. This would in turn have to bring contraction of the spinel-like block. Since the effect of contraction in the block due to comparative difference between ferrous and ferric ions in the ionic radii is nearly equal to that of expansion due to difference between ferric and zinc ions, the a axis of zinc-doped potassium ferrite would not vary with varying zinc content. Figure 6 shows the observed lattice parameters of the sample. It is clear that the a remains constant over the whole composition in agreement with the above discussion. Further, replacement of the ions might result in relative decrease of the ferrous ion concentration and decrease of the electronic conductivity of the sample.

3.5. Potassium Ion Conduction

As the divalent metal ion content is increased, the number of excess potassium ions will increase in accordance with the chemical formula $(1+x/2)K_2O\cdot 6Fe_2O_3\cdot xMeO$, and they will take up mid-oxygen sites rather than the BR sites (*20*). This increase in concentration of conductive species could result in an increase in the ionic conductivity. On the other hand, according to a model proposed by Roth (*21*) in which the charge-compensating defect is an oxygen interstitial in the mirror plane which would be expected to hinder alkali ion conduction, the increase in the cation concentration in potassium ferrites would lead to a decrease in the ionic conductivity. The effect to increase the ionic conductivity and the effect to decrease it might cancel each other.

Potassium ion conductivities of three potassium ferrites obtained from the total conductivities and the potassium ion transport numbers are shown in Fig. 7. The

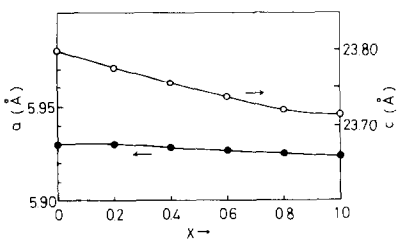

FIG. 5. Lattice parameters of nickel-doped potassium ferrite.

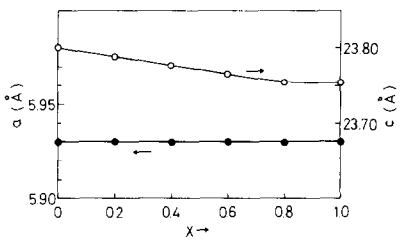

FIG. 6. Lattice parameters of zinc-doped potassium ferrite.

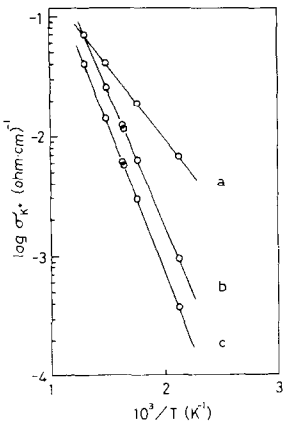

FIG. 7. Potassium-ion conductivities of the samples. (a) $K_2O{\cdot}6Fe_2O_3$, (b) $1.4K_2O{\cdot}6Fe_2O_3{\cdot}0.8ZnO$, (c) $1.5K_2O{\cdot}6Fe_2O_3{\cdot}NiO$.

undoped sample has the highest conductivity of the three and the slope of the curve is the lowest. Apparent activation energies for potassium ion conduction estimated from the slopes of the curves were 25.0, 45.1, and 50.6 kJ·mole^{-1} for undoped, zinc-doped, and nickel-doped potassium ferrite, respectively. Although the apparent activation energies for doped samples are slightly higher than that for the undoped sample, the value of 25.0 kJ·mole^{-1} for the undoped sample is in good agreement with the values of 25.5 ± 4.2 kJ·mole^{-1} found by Roth and Romanczuk (*9*) and 25.0 ± 2.5 kJ·mole^{-1} obtained by Dudley and Steele (*11*). These values are comparable to the activation energy 30.1 kJ·mole^{-1} for potassium ion self-diffusion in the mixed alkali ferrite phase (*14*). From these results it is confirmed that the migration of potassium ion in the hexagonal layer structure easily takes place, which is analogous to the sodium ion migration in sodium β-alumina.

In order to analyze the difference in the activation energies for potassium ion conduction, the potassium–oxygen layer width, l, was estimated using the equation described in earlier papers (*22*): $l = c/2 - [(22.49/2 - 4.76) + (a - 5.59)]$, where

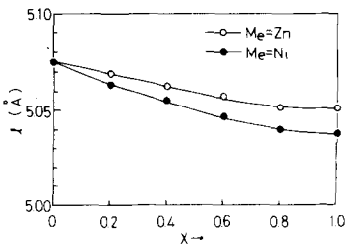

FIG. 8. Alkali–oxygen slot widths of doped specimens, $(1 + x/2)K_2O{\cdot}6Fe_2O_3{\cdot}xMeO$.

a and c are lattice parameters of the sample. In the calculation, the difference in density from sample to sample was ignored because it is fairly small. Further, isotropic contraction or expansion in the spinel-like block was assumed on the basis of cubic close packing of oxygen ions in the spinel structure. Figure 8 shows the layer width in nickel- and zinc-doped potassium ferrites. The layer width decreased a little with content of nickel or zinc oxide. This might impede the migration of the potassium ion in raising the activation energy compared with that in undoped potassium ferrite. In two doped samples the normal relation between the layer width and the activation energy can be seen from Fig. 8, namely, the wider the width, the lower the activation energy.

4. Conclusion

Electronic and ionic conductions in three kinds of potassium ferrites, $K_2O{\cdot}6Fe_2O_3$, $(1 + x/2)K_2O{\cdot}6Fe_2O_3{\cdot}xNiO$ $(0 < x \leq 1.0)$, and $(1 + x/2)K_2O{\cdot}6Fe_2O_3{\cdot}xZnO$ $(0 < x \leq 0.9)$, with β-alumina structure were investigated. The electronic conduction in the doped potassium ferrites would vary with the changes of ferrous ion concentration corresponding to the structural changes in the spinel-like blocks. The variations of ionic conductivities are explained qualitatively by the changes of the potassium–oxygen layer width accompanied by the dopings.

References

1. V. ADELSKOLD, *Ark. Kemi Min. Geol. A* **12**, 9 (1938).
2. V. CIRILLI AND C. BRISI, *Gazz. Chim. Ital.* **81**, 50 (1951).
3. E. W. GORTER, *Philips Res. Rep.* **9**, 363 (1954).
4. P. BRAUN, *Philips Res. Rep.* **12**, 491 (1957).
5. Y. OHTSUBO AND K. YAMAGUCHI, *Nippon Kagaku Zasshi* **82**, 676 (1961).
6. R. SCHOLDER AND M. MANSMANN, *Z. Anorg. Allg. Chem.* **321**, 246 (1963).
7. C. J. M. ROOYMANS, C. LANGEREIS, AND J. A. SCHULKES, *Solid State Commun.* **4**, 85 (1965).
8. T. TAKAHASHI, K. KUWABARA, AND Y. KASE, *Denki Kagaku* **43**, 273 (1975).
9. W. L. ROTH AND R. J. ROMANCZUK, *J. Electrochem. Soc.* **116**, 975 (1969).
10. G. J. DUDLEY, B. C. H. STEELE, AND A. T. HOWE, *J. Solid State Chem.* **18**, 141 (1976).
11. G. J. DUDLEY AND B. C. H. STEELE, *J. Solid State Chem.* **21**, 1 (1977).
12. T. TAKAHASHI, K. KUWABARA, AND Y. KASE, *Nippon Kagaku Kaishi* 1305 (1975).
13. K. KUWABARA AND T. TAKAHASHI, *J. Solid State Chem.* **19**, 147 (1976).
14. K. O. HEVER, *J. Electrochem. Soc.* **115**, 826 (1968).
15. K. O. HEVER, *J. Electrochem. Soc.* **115**, 830 (1968).
16. J. H. KENNEDY AND A. F. SAMMELS, *J. Electrochem Soc.* **121**, 1 (1974).
17. M. S. WHITTINGHAM AND R. A. HUGGINS, *J. Chem. Phys.* **54**, 414 (1971).
18. E. J. W. VERWEY AND E. L. HEILMANN, *J. Chem. Phys.* **15**, 174 (1947).
19. R. D. SHANNON AND C. T. PREWITT, *Acta Crystallogr. B* **25**, 925 (1969).
20. C. PETERS, M. BETTMAN, J. MOORE, AND M. GLICK, *Acta Crystallogr. B* **27**, 1826 (1971); J. C. WANG, M. GAFFARI, AND SANG-IL CHOI, *J. Chem. Phys.* **63**, 772 (1975).
21. W. L. ROTH, "GE Research Report 74 CRDO54" (1974).
22. K. KUWABARA AND T. TAKAHASHI, *J. Phys. Chem. Solids* **38**, 407 (1977); *J. Appl. Electrochem.* **7**, 339 (1977).